PHYSICAL REVIEW B **90**, 064408 (2014)

Voids-driven breakdown of the local-symmetry and Slater-Pauling rule in half-metallic Heusler compounds

I. Galanakis,[1,*] E. Şaşıoğlu,[2,†] S. Blügel,[2] and K. Özdoğan[3,‡]
[1]*Department of Materials Science, School of Natural Sciences, University of Patras, GR-26504 Patra, Greece*
[2]*Peter Grünberg Institut and Institute for Advanced Simulation, Forschungszentrum Jülich and JARA, 52425 Jülich, Germany*
[3]*Department of Physics, Yildiz Technical University, 34210 İstanbul, Turkey*
(Received 20 June 2014; revised manuscript received 23 July 2014; published 8 August 2014)

Slater-Pauling (SP) rules connect the magnetic and electronic properties of the half-metallic (HM) Heusler compounds. Employing first-principles electronic structure calculations we explore the validity of the SP rules in the case of transition from HM semi-Heusler compounds to various cases of HM full-Heusler compounds. We show that the coherent-potential approximation yields half-metallicity and thus a generalized version of the SP rules can be derived. On the contrary, supercell calculations, which are expected to describe the experimental situation more accurately, show that the energy gap considerably shrinks for the intermediate compounds and in several cases the half-metallicity is completely destroyed. The origin of this behavior is attributed to the voids, which influence the symmetry of the lattice.

DOI: 10.1103/PhysRevB.90.064408 PACS number(s): 75.50.Cc, 75.30.Et, 71.15.Mb

I. INTRODUCTION

The research on magnetic nanomaterials and their incorporation in functional devices is a central issue in modern electronics and consequently the field of spintronics, where both magnetic and semiconducting elements are combined, and of magnetoelectronics (incorporating exclusively magnetic elements) are rapidly developing [1]. Half-metallic (HM) magnetic compounds play a crucial role in this development [2]. These materials present usual metallic behavior for the one spin direction while an energy gap in the band structure is present in the other spin direction similarly to semiconductors [3]. The possibility of creating 100% spin-polarized current and their potential advantages in electronic devices has triggered the interest on such compounds [4,5]. De Groot and collaborators in 1983 have initially suggested based on electronic structure calculations that NiMnSb, a semi-Heusler compound, is a half-metal [6] and since then several HM compounds have been discovered [7,8]. Several aspects concerning the implementation of HM compounds in realistic devices, like tunneling magnetic junctions or giant magnetoresistive junctions and spin injectors, have been discussed in literature (see Ref. [4] for a review).

Heusler compounds are a promising family to achieve half-metallicity since they encompass a large number of members. Most of them crystallize in cubic structures similar to the zincblende structure of semiconductors and several have very high Curie temperatures [9,10]. Computational materials science has played a crucial role in the design of HM Heusler compounds and several have been initially predicted and half-metallicity was later experimentally confirmed [3]. The lattice for all Heusler compounds is an fcc with four equidistant sites as basis along the diagonal of the unit cell. In Fig. 1, we give a schematic representation of the various structures of the Heusler compounds. The first family are the so-called semi-Heuslers, which have the chemical formula XYZ where the sequence of the sites along the diagonal is X-Y-void-Z. The X and Y are transition-metal elements and Z is an sp element and the structure is known as the $C1_b$ lattice [9]. The second family consists (i) of the usual full-Heusler compounds with the chemical formula X_2YZ, where the valence of the X is larger than Y [known as the $L2_1$ structure illustrated in Fig. (1)], (ii) the inverse Heuslers when the valence of the Y elements is the largest and the compounds crystallize in the so-called XA structure where the sequence of the atoms changes, and finally, (iii) the ordered quaternary LiMgPdSn-type compounds with chemical type $(XX')YZ$ where the valence of X and X' is larger than that of Y [9,10].

In two pioneering papers, Slater and Pauling have shown that in the case of binary magnetic compounds when one valence electron is added to the compound, this occupies spin-down states only and the total spin magnetic moment decreases by about $1\mu_B$ [11,12]. Interestingly, a similar behavior can be also found in HM magnets as confirmed by first-principles (*ab initio*) electronic structure calculations. In HM Heusler compounds, the spin-down band structure is fixed; the number of spin-down occupied bands and their character does not change within the HM members of the same family of compounds. The extra valence electrons now occupy exclusively spin-up states. These Slater-Pauling (SP) rules connect the electronic properties (appearance of the HM behavior) directly to the magnetic properties (total spin magnetic moments) and thus offer a powerful tool to the study of HM compounds since (i) magnetic measurements can be used to confirm the HM character of a compound and (ii) simple valence electrons counting can predefine the magnetic properties of a half-metal. However, in realistic situations, the vacant site of the semi-Heusler compounds (see Fig. 1) can be partially occupied as in Mn_2Ru_xGa films recently studied [13]. Thus the question rises if half-metallicity is present and SP rules exist for such compounds being in-between the semi- and full-Heuslers. In this paper, we have studied six such families where the end compound ($x = 1$) belongs to another subfamily of full-Heuslers: (i) $Co_{1+x}CrSi$ and $Co_{1+x}MnSi$ (end compounds usual full-Heuslers), (ii) $(Co_xFe)MnSi$

*galanakis@upatras.gr
†e.sasioglu@fz-juelich.de
‡kozdogan@yildiz.edu.tr

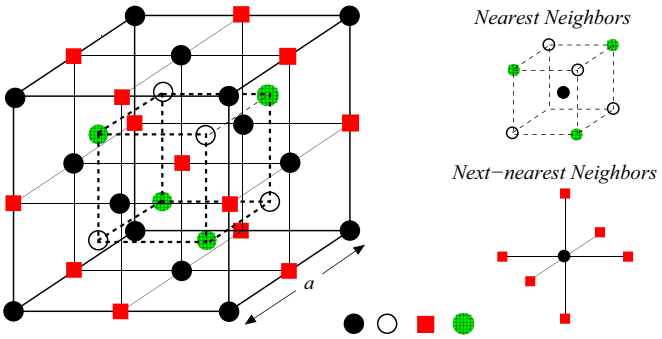

	A	B	C	D
Semi−Heuslers ($C1_b$) : XYZ	X	Y		Z
Full−Heuslers ($L2_1$) : X_2YZ	X	Y	X	Z
Quaternary Heuslers : (XX')YZ	X	Y	X'	Z
Inverse Heuslers (XA) : X_2YZ	X	X	Y	Z

FIG. 1. (Color online) Schematic representation of the various structures of Heusler compounds. On the right we present the nearest and next-nearest neighbors of an A site. Note that the large cube contains exactly four primitive unit cells.

and (CoFe$_x$)MnSi (LiPdMgSn-type full-Heuslers), and (iii) $Mn_{2+x}Si$ and Mn_2Co_xSi (inverse full-Heuslers). We have used for all six cases the lattice constant of Co_2MnSi of 5.65 Å [9]. We have considered the $x = 0$, 0.25, 0.5 0.75, and 1.0 values of the concentration. We have employed the full-potential nonorthogonal local-orbital minimum-basis band-structure scheme (FPLO) [14] within the local-spin density approximation (LSDA) [15]. To simulate disorder at the C site we employ first the coherent-potential approximation (CPA) [16]. In CPA each C site is partially occupied with a probability given by the respective concentration of the corresponding chemical type. However, the CPA method does not take into account the short-range correlations since in CPA the real crystal is replaced by a fictitious one. In reality this is not true and we performed supercell (SC) calculations to examine this effect considering the large cube presented in Fig. 1 to account for the fractional concentration at the C sites.

II. RESULTS AND DISCUSSION

Before presenting calculational results, we will shortly discuss the origin of the SP rules in Heusler compounds since this is crucial for the discussion of the findings. The reader is referred to Refs. [17–20] for further details. In the case of semi-Heuslers (XYZ), the role of the *sp* element is to provide in the spin-down electronic band structure a single *s* and a triple-degenerated *p* band deep in energy [17]. The *d* orbitals of the two transition metal atoms hybridize strongly creating five occupied bonding and five unoccupied antibonding *d* states in the spin-down band structure (see upper panel in Fig. 2) [17]. Each set of five *d* hybrids contains the double degenerate e_g and the triple degenerate t_{2g} states. As a result there are in total exactly nine occupied spin-down states and the SP relation is $M_t = Z_t - 18$, where M_t is the total spin magnetic moment in μ_B and Z_t the total number of valence electrons [17]. In the case of usual full-Heuslers (X_2YZ), the situation is more complicated due to the presence of the second X atom. Although the symmetry of the $L2_1$ lattice is the tetrahedral one, the X elements themselves, if we neglect the Y and Z

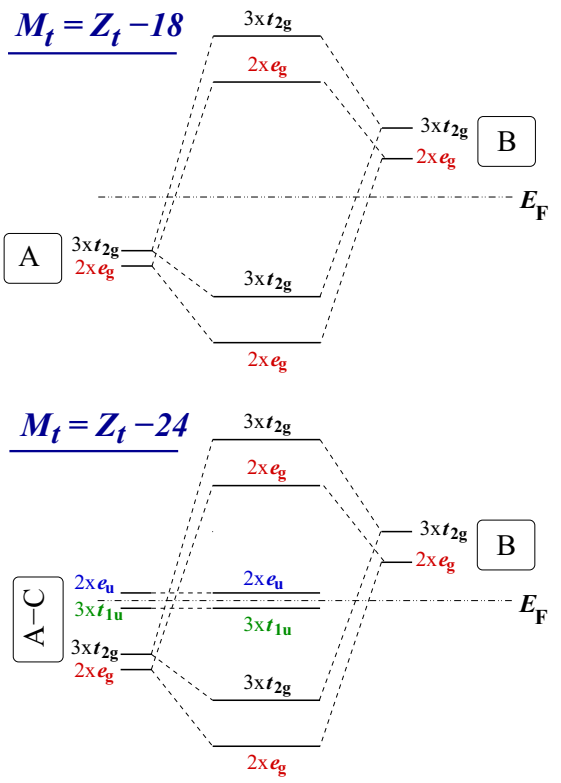

FIG. 2. (Color online) Schematic representation of the hybridization between the *d* valence orbitals of the transition-metal atoms in half-metallic Heusler compounds in the presence of two (upper panel) or three (lower panel) transition metal atoms in the primitive unit cell.

atoms, form a simple cubic lattice and sit at sites of octahedral symmetry (see Fig. 1 for an illustration of the nearest and next-nearest neighbors) [18]. The *d* orbitals of the neighboring X atoms at the A and C sites hybridize creating five bonding *d* states, which after hybridize with the *d* orbitals of the Y atoms creating five occupied and five unoccupied *d* hybrids, and five nonbonding *d* hybrids of octahedral symmetry (the triple-degenerate t_{1u} and double-degenerate e_u states). These hybridizations are schematically drawn in the lower panel of Fig. 2. These nonbonding hybrids cannot couple with the orbitals of the neighboring atoms, since they do not obey the tetrahedral symmetry, and only the t_{1u} are occupied leading to a total of 12 occupied spin-down states and the SP relation is now $M_t = Z_t - 24$ [18]. A similar SP rule stands also for the inverse HM compounds, where X = Mn or Cr [19], and the ordered quaternary LiMgPdSn-type Heuslers [20]. The SP rule $M_t = Z_t - 24$ for full Heuslers also holds in the case of disordered quaternary and quinternary full-Heusler compounds where all sites of the lattice are fully occupied [21–23].

We now return to the discussion of the obtained results. For all six studied cases, we present in Fig. 3 the calculated total spin magnetic moments (in μ_B) expressed per formula unit both within CPA and SC approaches. In all cases, CPA results are exactly on top of the straight line connecting the total spin magnetic moments for the ordered end compounds. Thus the total spin moment in CPA scales linearly with the concentration x at the C site following a generalized version of the SP rule $M_t = Z_t - (18 + 6x)$ so that for $x = 0$ and

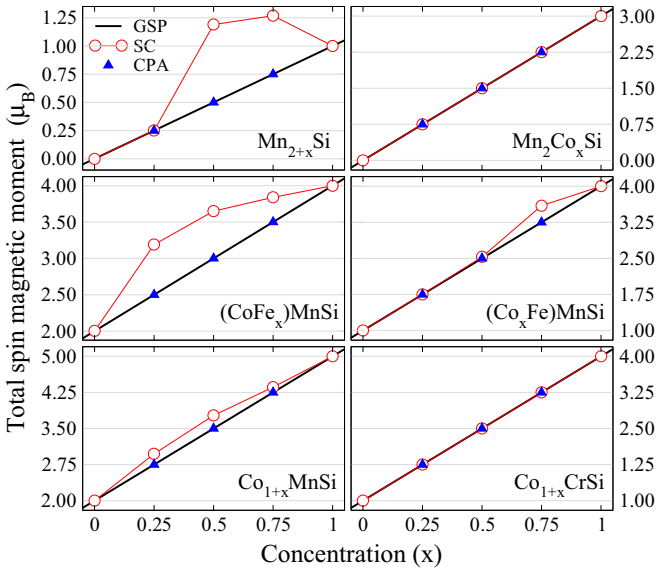

FIG. 3. (Color online) Total spin magnetic moment (in μ_B) per formula unit as a function of the concentration of the atoms at the C site within both CPA and SC approximations for all studied transitions. Note that CPA results follow a generalized version of the SP rule, $M_t = Z_t - (18 + 6x)$, in all cases.

1, we obtain the $M_t = Z_t - 18$ and $Z_t - 24$ SP rules, for the semi- and full-Heusler compounds, respectively. This is a sign that within CPA all compounds remain half-metallic throughout the transition. However, CPA does not represent the actual experimental situation since artificially we occupy the C site by a fractional atom. On the other hand, SC approach takes into account the short-range correlations since the C sites are either occupied or empty. These voids within the SC calculations break the octahedral symmetry discussed above since the occurrence of t_{1u} and e_u states is based on the fact that all six next neighbors of the A sites (see Fig. 1) are occupied to form a cubic lattice made up from the A and C sites. Thus within the SC approach it is not by definition that the total spin magnetic moment should scale with the concentration x, neither that half-metallicity is preserved. For the three compounds $Co_{1+x}MnSi$, $(CoFe_x)MnSi$, and $Mn_{2+x}Si$ the CPA and SC total magnetic moments are quite different, especially for the last compound. For the $Co_{1+x}CrSi$ and $Mn_{1+x}CoSi$ compounds, the total magnetic moment within SC approach follows the SP rule as for the SC calculations for $Cr_{2+x}Se$ presented in Ref. [24], while for $(Co_xFe)MnSi$, there is a deviation only for $x = 0.75$. Thus within the SC approximation no general conclusion can be drawn regarding the half-metallicity and the corresponding SP behavior of the compounds under study. We should, finally, also note that the atomic spin magnetic moments do not present any peculiarity and scale linearly as the concentration x increases between the two extreme compounds; in Table I, we present the $Co_{1+x}MnSi$ case but results are similar for all other studied compounds.

To elucidate the origin of these discrepancies, we plot in Fig. 4 the total density of states (DOS) per formula unit for the $Co_{1+x}MnSi$ and $Co_{1+x}CrSi$ compounds, since in the former CPA and SC, calculated spin magnetic moments deviate and in the later they coincide; the other four families of compounds

TABLE I. Atom-resolved spin magnetic moments (in μ_B) for the transition metal elements of the $Co_{1+x}MnSi$ compounds as a function of the Co concentration at the C site. Note that within the supercell there are four Co atoms at the A sites. Not all Co atoms are equivalent and thus we give all calculated Co^A spin moments, where the numbers in parenthesis denote the number of Co^A atoms with the same spin magnetic moment. As a rule of thumb for the same value of x the Co^A atoms with the largest number of Co^C next-nearest neighbors have the largest spin magnetic moment.

$Co_{1+x}MnSi$	Co^A		Mn^B		Co^C	
x	CPA	SC	CPA	SC	CPA	SC
0		−0.33		2.59		
0.25	−0.13	0.08 (3)	2.84	2.92	0.73	1.04
		−0.20 (1)				
0.50	0.35	0.55 (2)	2.89	3.05	0.79	0.98
		0.28 (2)				
0.75	0.76	0.67 (3)	2.91	3.08	0.92	0.95
		0.87 (1)				
1		0.99		3.12		0.99

present identical behavior concerning the minority-spin energy gap. For the perfect compounds in the top panels, they all present pretty large HM energy gaps (this is the reason we have chosen as Z the Si atom since these compounds present in general much larger gaps and it is easier to see any influence

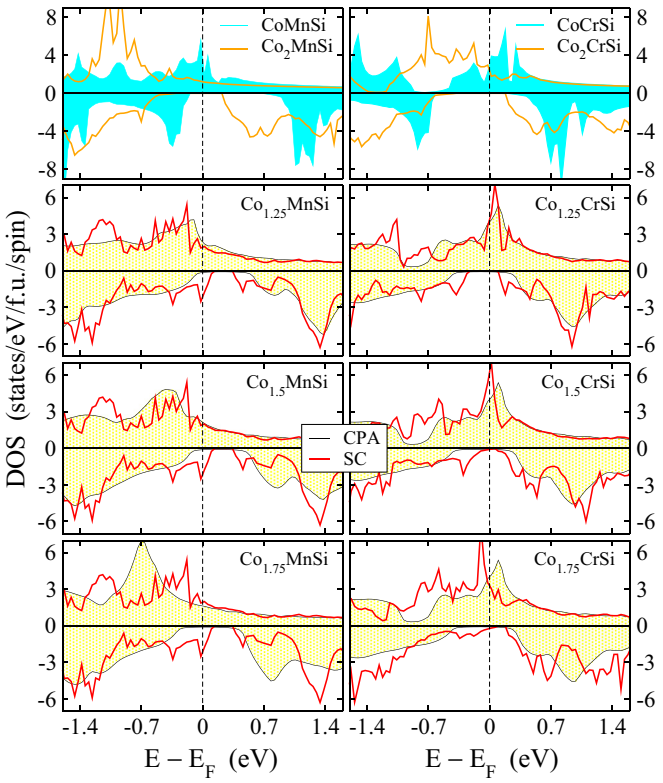

FIG. 4. (Color online) Total DOS for the $Co_{1+x}MnSi$ (left) and $Co_{1+x}MnSi$ (right) for all studied concentrations using both CPA and SC approximations. The upper graphs correspond to the end compounds.

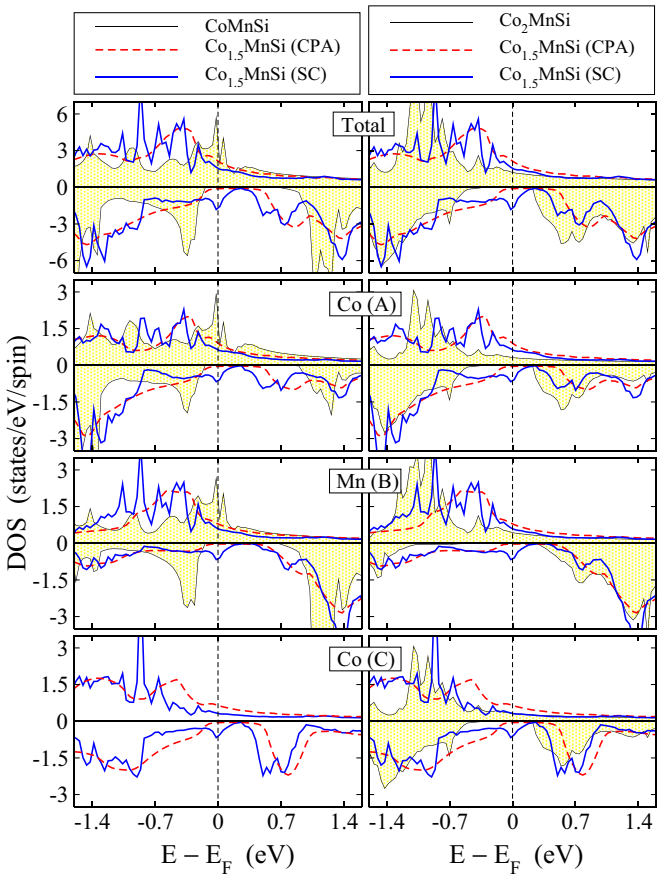

FIG. 5. (Color online) Comparison of the total and atom resolved DOS for the $Co_{1.5}MnSi$ compound with CoMnSi (left panels) and Co_2MnSi (right panels). With red (blue) lines the CPA (SC) results are shown. Note that within SC calculations for Co at the A site we present the DOS for the Co atom with spin magnetic moment $0.55\mu_B$ (see Table I). The other Co(A) atom with spin moment $0.28\mu_B$ presents similar minority-spin DOS around the Fermi level.

on the gap properties) [18]. The difference is that for CoMnSi and Co_2MnSi there is an offset of the energy gaps while for CoCrSi and Co_2CrSi the energy gap almost coincide. Within CPA the doping with extra Co atoms at the C site keeps the half-metallicity and there is a gap in the energy region where the gaps of the two end compounds overlap. Within SC as we start adding Co at the C sites new states emerge at the edge of the gap of the perfect CoMnSi and CoCrSi compounds and the gap considerably shrinks for both families of compounds. In the case of CoMnSi, the Fermi level is close to the left edge of the gap and for $Co_{1+x}MnSi$ ($x = 0.25, 0.5, 0.75$) it crosses these states, while in the case of CoCrSi the Fermi level is located at the middle of the gap and thus for $Co_{1+x}CrSi$ ($x = 0.25, 0.5, 0.75$) it remains within the gap without crossing the states that appear at the edges of the gap. These new states within the SC simulations are spread throughout the whole crystal as can be deduced from the atom-resolved DOS; as a representative example we provide the atom-resolved DOS for $Co_{1.5}MnSi$ in Fig. 5 but results are similar for all compounds and for all intermediate concentrations. For $x = 1$, the emergence of octahedral symmetry allows the creation of the t_{1u} and e_u states and there is an abrupt transition towards a new much broader energy gap. Thus in reality, there is no fundamental difference in the behavior of the studied compounds in terms of gap properties and small details in the DOS (exact position of the Fermi level for the $x = 0$ case) determine whether the half-metallicity is conserved or not. In the cases where half-metallicity is lost, the generalized $M_t = Z_t - (18 + 6x)$ SP rule breaks also down.

Finally, we should stretch the fact that in the case of semiconductors, it is well known that the introduction of defects such as voids breaks the symmetry of the crystal structure destroying the periodicity of certain bands and thus creating localized electronic states right in the gap since these states are not hybridized and thus do not form a band. In the case of Heusler compounds under study, contrary to semiconductors where the band structure is identical for both spin directions, it may occur that these states due to the voids are not located right in the middle of the minority-spin energy gap but at its edges keeping the half-metallic character of the parent compounds. This differs the half-metallic compounds under study, which have an energy gap only in one spin direction from the usual semiconductors.

III. SUMMARY AND CONCLUSIONS

We have performed first-principles electronic structure calculations to study the transition from HM semi-Heusler compounds to HM full-Heusler compounds by doping the C site by transition metal atoms (see Fig. 1). CPA method gives a linear variation of the total spin magnetic moment keeping the half-metallic character and leads to a generalized version of the SP rule for half-metallic Heusler compounds: $M_t = Z_t - (18 + 6x)$, where M_t is the total spin magnetic moment in the formula unit cell (in μ_B), Z_t the total number of valence electrons, and x the fractional population at the C site. We have shown that the CPA ignores short-range correlations and thus SC calculations turned out to be more suitable to describe the experimental situation. In the latter, the occurrence of voids at the C sites destroys the octahedral symmetry of the A and C sites observed in full-Heusler compounds and thus leads to states at the edges of the minority-spin gap and thus to a considerable shrinking of the gap. Whether the half-metallicity is preserved or not within the SC calculations depends on the initial position of the Fermi level in the semi-Heusler end compound. If the Fermi level is located at the edges of the gap for the semi-Heusler, then the half-metallicity is lost for the intermediate compounds and the generalized SP rule is no more obeyed. When all C sites are occupied and we transit abruptly to the end full-Heusler compounds the gap again reopens and half-metallicity is restored. Present findings should lead to an understanding of the experimental data on films of Heusler compounds where only a fraction of the C sites is occupied and should considerably contribute to the further development of magnetic nanomaterials for spintronics/magnetoelectronics applications.

ACKNOWLEDGMENTS

I.G. acknowledges that this research has been co-financed by the European Union (European Social Fund - ESF) and Greek national funds through the Operational Program

Education and Lifelong Learning of the National Strategic Reference Framework (NSRF) - Research Funding Program: ARISTEIA II. Investing in knowledge society through the European Social Fund.

[1] I. Žutić, J. Fabian, and S. Das Sarma, Rev. Mod. Phys. **76**, 323 (2004).
[2] M. I. Katsnelson, V. Yu. Irkhin, L. Chioncel, A. I. Lichtenstein, and R. A. de Groot, Rev. Mod. Phys. **80**, 315 (2008).
[3] T. Graf, C. Felser, and S. S. P. Parkin, Prog. Solid State Chem. **39**, 1 (2011).
[4] A. Hirohata and K. Takanashi, J. Phys. D: Appl. Phys. **47**, 193001 (2014).
[5] K. Sato, L. Bergqvist, J. Kudrnovský, P. H. Dederichs, O. Eriksson, I. Turek, B. Sanyal, G. Bouzerar, H. Katayama-Yoshida, V. A. Dinh, T. Fukushima, H. Kizaki, and R. Zeller, Rev. Mod. Phys. **82**, 1633 (2010).
[6] R. A. de Groot, F. M. Mueller, P. G. van Engen, and K. H. J. Buschow, Phys. Rev. Lett. **50**, 2024 (1983).
[7] W. E. Pickett and H. Eschrig, J. Phys.: Condens. Matter **19**, 315203 (2007).
[8] M. Meinert, Phys. Rev. B **87**, 045103 (2013).
[9] P. J. Webster and K. R. A. Ziebeck, in *Alloys and Compounds of d-Elements with Main Group Elements. Part 2*, edited by H. R. J. Wijn, Landolt-Boörnstein, New Series, Group III, Vol. 19, Pt.c (Springer-Verlag, Berlin, 1988), pp. 75–184.
[10] K. R. A. Ziebeck and K.-U. Neumann, in *Magnetic Properties of Metals*, edited by H. R. J. Wijn, Landolt-Börnstein, New Series, Group III, Vol. 32/c (Springer, Berlin, 2001), pp. 64–414.
[11] J. C. Slater, Phys. Rev. **49**, 931 (1936).
[12] L. Pauling, Phs. Rev. **54**, 899 (1938).
[13] H. Kurt, K. Rode, P. Stamenov, M. Venkatesan, Y.-C. Lau, E. Fonda, and J. M. D. Coey, Phys. Rev. Lett. **112**, 027201 (2014).
[14] K. Koepernik and H. Eschrig, Phys. Rev. B **59**, 1743 (1999).
[15] J. P. Perdew and Y. Wang, Phys. Rev. B **45**, 13244 (1992).
[16] K. Koepernik, B. Velický, R. Hayn, and H. Eschrig, Phys. Rev. B **55**, 5717 (1997).
[17] I. Galanakis, P. H. Dederichs, and N. Papanikolaou, Phys. Rev. B **66**, 134428 (2002).
[18] I. Galanakis, P. H. Dederichs, and N. Papanikolaou, Phys. Rev. B **66**, 174429 (2002).
[19] S. Skaftouros, K. Özdoğan, E. Şaşıoğlu, and I. Galanakis, Phys. Rev. B **87**, 024420 (2013).
[20] K. Özdoğan, E. Şaşıoğlu, and I. Galanakis, J. Appl. Phys. **113**, 193903 (2013).
[21] I. Galanakis, J. Phys.: Condens. Matter **16**, 3089 (2004).
[22] K. Özdoğan, B. Aktaş, I. Galanakis, and E. Şaşıoğlu, J. Appl. Phys. **101**, 073910 (2007).
[23] K. Özdoğan, E. Şaşıoğlu, and I. Galanakis, J. Appl. Phys. **103**, 023503 (2008).
[24] I. Galanakis, K. Özdoğan, and E. Şaşıoğlu, Phys. Rev. B **86**, 134427 (2012).